

# Synthesis, crystal structure and hydrogenation properties of the novel metal compound $\text{LaNi}_2\text{Mn}_3$

L. Guénee, K. Yvon\*

Laboratoire de Cristallographie, Université de Genève, 24 Quai E. Ansermet, CH-1211 Genève 4, Switzerland

Received 24 May 2002; accepted 4 June 2002

## Abstract

$\text{LaNi}_2\text{Mn}_3$  has been synthesised from the elements and investigated with respect to crystal structure and hydrogenation properties. Single crystal X-ray diffraction reveals a  $\text{YNi}_2\text{Al}_3$  type structure (space group  $P6/mmm$ ,  $a=9.2099(9)$ ,  $c=4.1892(4)$  Å,  $c/a=0.4548$ ) that is distinctly different from the  $\text{CaCu}_5$  type structure of  $\text{LaNi}_5$ . The compound absorbs reversibly up to six hydrogen atoms per formula unit near ambient conditions and shows a hydrogen plateau pressure of  $\sim 1$  bar near  $60^\circ\text{C}$ . The hydrogen atoms in the expanded metal atom structure were localised by neutron powder diffraction on deuterides of composition  $\text{LaNi}_2\text{Mn}_3\text{D}_{4.6}$  ( $a=9.7125(2)$ ,  $c=4.3057(1)$  Å,  $c/a=0.4433$ ) and  $\text{LaNi}_2\text{Mn}_3\text{D}_{5.6}$  ( $a=9.8379(2)$ ,  $c=4.3038(1)$ ,  $c/a=0.4375$ ). They occupy one octahedral coordinated site  $[\text{La}_2\text{Mn}_4]$  with full occupancy and three tetrahedral coordinated sites  $[\text{La}_2\text{Mn}_2]$ ,  $[\text{La}_2\text{NiMn}]$  and  $[\text{LaMn}_2\text{Ni}]$ , and a deformed square pyramidal coordinated site  $[\text{LaMn}_2\text{Ni}_2]$  with partial occupancies.

© 2002 Elsevier Science B.V. All rights reserved.

Keywords: Hydrogen absorbing materials; Metal hydrides; Crystal structure; Neutron diffraction

## 1. Introduction

Intermetallic  $\text{LaNi}_5$  and its substitution derivatives are of interest for applications in rechargeable batteries (for a recent review see Ref. [1]). The manganese substituted series  $\text{LaNi}_{5-x}\text{Mn}_x$  has been studied in detail in Ref. [2] and found to crystallise with a partially disordered  $\text{CaCu}_5$  type structure for manganese contents  $0 \leq x \leq 2.2$  ( $800^\circ\text{C}$ ). For higher manganese contents ( $x > 0.2$ ,  $600^\circ\text{C}$ ) a new ternary compound appeared in a phase diagram [3] the composition of which was stated to be  $\text{La}_3\text{Mn}_{10}\text{Ni}_7$ . A ternary compound of composition  $\text{LaNi}_2\text{Mn}_3$  and its hydrogenation properties have so far not been reported. A recent study of structure maps has shown [4] that this composition is outside the stability range of the  $\text{CaCu}_5$  type structure but inside that of the hexagonal  $\text{YNi}_2\text{Al}_3$  type structure (also called  $\text{HoNi}_{2.6}\text{Ga}_{2.4}$  type). The latter structure is ordered and closely related to, but significantly different from, the  $\text{CaCu}_5$  type structure. So far, only compounds based on aluminium, gallium and tin were found to crystallise with that structure, and they were

relatively poor hydrogen absorbers. The purpose of the present work was to synthesise a compound of composition  $\text{LaNi}_2\text{Mn}_3$ , to investigate its crystal structure and to study its hydrogenation properties. It will be shown that the compound crystallises with the expected  $\text{YNi}_2\text{Al}_3$  type structure and shows excellent hydrogen storage properties.

## 2. Experimental

### 2.1. Synthesis and hydrogenation properties

Samples were obtained by placing compressed powder mixtures of the elements (La rod (Johnson Matthey, 99.99%), Ni and Mn powders (Johnson Matthey, 5N) in an induction furnace and by re-melting them several times in a silver crucible under argon (6N). The ingots ( $\sim 1$  g) were then wrapped into Ta foils, placed into quartz ampoules that were sealed under 0.3 bar argon pressure, and annealed at various temperatures. In spite of negligible melting losses ( $< 0.1$  wt.%) initial attempts to obtain  $\text{LaNi}_2\text{Mn}_3$  as a single phase at the stoichiometric composition failed, even after long-time annealing of the samples at  $600$  or  $800^\circ\text{C}$ . The sample which was annealed at  $600^\circ\text{C}$  during 4 days, for example, contained a well-

\*Corresponding author. Tel.: +41-22-702-6231; fax: +41-22-702-6864.

E-mail address: klaus.yvon@cryst.unige.ch (K. Yvon).

crystallized majority phase that could be attributed to the hexagonal  $\text{YNi}_2\text{Al}_3$  type structure (space group  $P6/mmm$ , refined cell parameters  $a=9.19089(4)$ ,  $c=4.17861(4)$  Å) and two Ni(Mn)-rich secondary phases of likely composition  $\text{La}_2(\text{Ni,Mn})_{17}$  (rhombohedral  $\text{Th}_2\text{Zn}_{17}$  type structure) and  $\text{LaNi}_3\text{Mn}_6$  (tetragonal  $\text{CeNi}_5\text{Mn}_6$  type structure). On the other hand, the sample which was annealed at 800 °C during 24 h contained well crystallized  $\text{LaNi}_5\text{Mn}_6$  as a majority phase and traces of orthorhombic  $\text{LaNi}$  (CrB type structure) and possibly some  $\text{La}_2\text{O}_3$ , while the  $\text{LaNi}_2\text{Mn}_3$  and  $\text{La}_2(\text{Ni,Mn})_{17}$  phases had disappeared. In order to avoid the formation of these unwanted phases a lanthanum excess of up to 5 wt.% (nominal composition  $\text{La}_{1.07}\text{Ni}_2\text{Mn}_3$ ) was used during the subsequent syntheses and the samples were annealed between 600 and 630 °C for up to 11 days (see below). X-ray powder diffraction patterns showed these samples to be nearly single-phase, containing mainly  $\text{LaNi}_2\text{Mn}_3$  ( $\text{YNi}_2\text{Al}_3$  type structure), very little Mn(Ni) (~4 wt.%) and some traces of  $\text{La}_2\text{O}_3$  (<1 wt.%).

For the hydrogenation (deuteration) experiments various alloy samples were powdered in a glove box to an average grain size of 63 µm. One sample (~0.5 g mass) was filled into a Ni container and placed into an autoclave that was evacuated. The temperature was increased up to 80 °C while hydrogen was introduced to a pressure of 2 bar, and the temperature was kept at that level for one night. X-ray synchrotron patterns indicated that the hydride samples were nearly single-phase but tended to desorb hydrogen

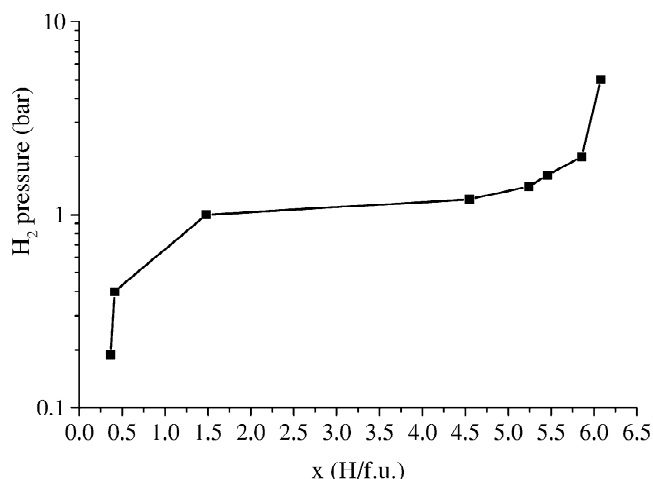


Fig. 2. Pressure-composition isotherm of  $\text{La}_{1.07}\text{Ni}_2\text{Mn}_3$  at  $T=60^\circ\text{C}$  in microbalance (composition corrected for 7 wt.% Mn, maximum H content 6.08 H/f.u.).

(see Section 2.2). Other samples (nominal composition  $\text{La}_{1.07}\text{Ni}_2\text{Mn}_3$ , ~0.05 g mass) were placed into a microbalance (Hidden Analytical, model IGA001) and hydrogenated at various temperatures (50–80 °C) and pressures (0.01–3 bar). As can be seen from Fig. 1 their absorption at 60 °C and 1.5 bar showed good kinetics and led to a maximum hydrogen content of about 6 H atoms per formula unit (H/f.u). The sample was not activated prior to the measurement. A pressure-composition isotherm at 60 °C for the same sample during absorption is presented in Fig. 2. It

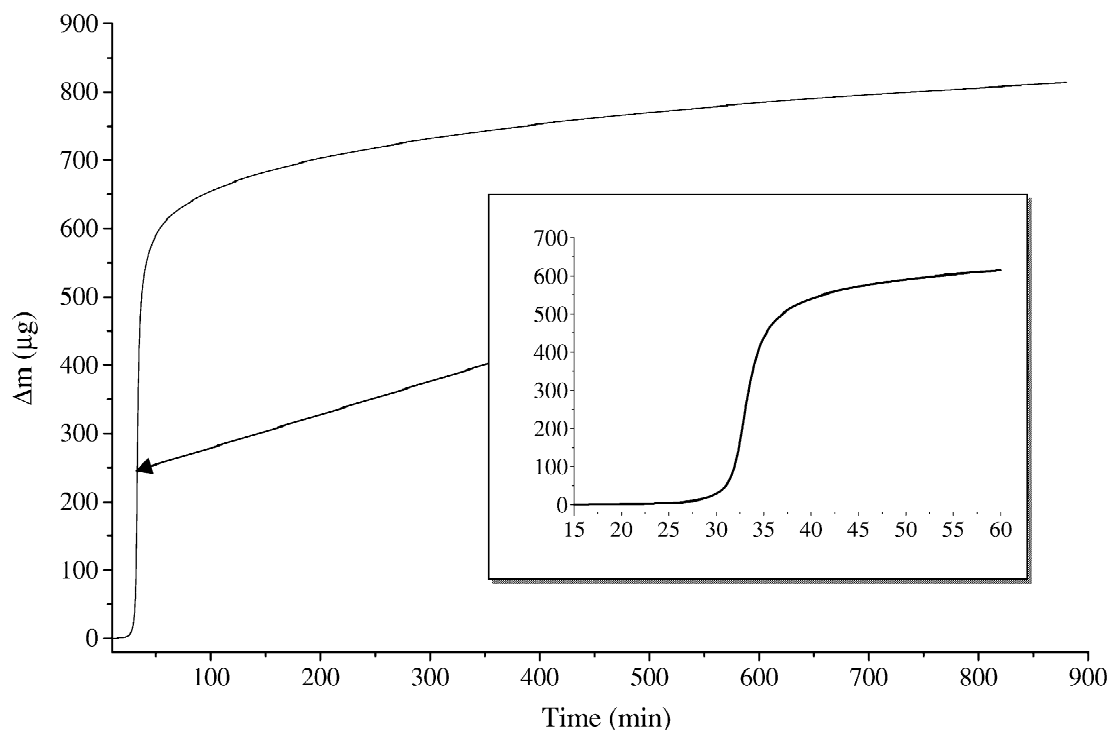


Fig. 1. Mass increase ( $\mu\text{g}$ ) versus time of  $\text{La}_{1.07}\text{Ni}_2\text{Mn}_3$  in microbalance,  $T=60^\circ\text{C}$ , 1.5 bars hydrogen pressure, initial sample weight 0.06113 g, total weight variation  $\Delta m=287.6$  µg, maximum hydrogen content 6.03 H/f.u., values corrected for the presence of 7 wt.% Mn impurity.

shows a rather well-defined plateau at  $\sim 1$  bar that extends to  $\sim 6$  H atoms per formula unit (H/f.u). The hydride was found to be stable at ambient temperature under a hydrogen pressure of  $< 1$  bar, but desorbed rapidly if exposed to air. Complete desorption without further oxidation and/or segregation occurred within 5 days.

## 2.2. Structure analysis

In order to study the structure of the alloy a single crystal was isolated from the bulk and measured on an X-ray diffractometer (STOE IPDS) equipped by an image plate (Mo  $K\alpha$  radiation). The absence of systematic extinctions confirmed space group  $P6/mmm$  and yielded the refined cell parameters  $a=9.2099(9)$  and  $c=4.1892(4)$  Å. A structure refinement (programme Xtal3.7 [5]) was performed (on  $F^2$ ) by placing La, Ni and Mn on the Y, Ni and Al sites, respectively, of the  $YNi_2Al_3$  type structure [6] and by varying one scale factor and 15 atomic parameters. Results are summarised in Table 1. A refinement of occupancy factors gave no indication for a possible disorder of Ni and Mn on the three atom sites. Finally, a phase analysis and structure refinement by using synchrotron X-ray data was made on a polycrystalline sample that was subsequently subjected to hydrogenation studies. The results showed that  $LaNi_2Mn_3$  was the majority phase (89 wt.%) and Mn(Ni) (6.7 wt.%), LaNi (1.5 wt.%) and  $La_2O_3$  (2.7 wt.%) minority phases. Compared to the single crystal results no significant structural differences were observed for the  $LaNi_2Mn_3$  phase except for slightly smaller cell parameters ( $a=9.20179(7)$ ,  $c=4.18078(4)$  Å).

For the study of the hydride structure a hydrogenated sample was first measured by synchrotron radiation. The metal atom substructure of the majority phase was found to

remain of the  $YNi_2Al_3$  type but showed a considerable lattice expansion ( $a=9.8951(3)$ ,  $c=4.3061(1)$  Å,  $\Delta V/V=18.7\%$ ) compared to the alloy. Furthermore, the expansion was anisotropic as shown by the cell parameter ratios  $c/a=0.4351$  (hydride) and 0.4544 (alloy). Unfortunately, the partial hydrogen desorption and the resulting sample inhomogeneity prevented the metal atom substructure from being refined. Subsequently, a deuterated sample ( $\sim 7$  g mass) was prepared by deuteration of three alloy batches of nominal composition  $La_{1.04}Ni_2Mn_3$  in an autoclave (4.5 bar,  $T=65$  °C, 12 h). Prior to the experiment the alloys were annealed at 630 °C for 11 days, finely ground and sieved (grain size  $< 64$   $\mu m$ ). A quantitative X-ray phase analysis showed that they contained mainly the  $LaNi_2Mn_3$  phase (96 wt.%) and some Mn(Ni) (4 wt.%). After the deuteration reaction was completed, the sample (called **I**) was filled into a vanadium container under protective atmosphere (1 bar argon) and measured on the neutron powder diffractometer HRPT ( $\lambda=1.494$  Å) at SINQ (PSI, Villigen). As expected, the main phase had a strongly expanded hexagonal cell ( $a=9.7125(2)$ ,  $c=4.3057(1)$  Å) and the concentration of the secondary Mn(Ni) phase was nearly the same as in the starting material. Five deuterium sites in the metal atom substructure of the main phase were located ab initio by the program FOX [7] and their coordinates refined by the programme Fullprof [8]. The following 32 parameters were allowed to vary: two scale factors, five profile and 25 atomic parameters. The patterns are presented in Fig. 3 and the refinement results are summarised in Table 2. After completing the experiment, sample **I** was again placed in an autoclave, deuterated at a slightly higher temperature and pressure ( $T=75$  °C, 6 bar, 12 h), and re-measured on the neutron powder diffractometer D1A ( $\lambda=1.9114$  Å) at ILL (Grenoble). As expected, this new sample (called **II**) contained a more deuterium-

Table 1  
Structure refinement results on a single crystal of  $LaNi_2Mn_3$ ; e.s.d.s in parentheses

Atoms	Site	x	y	z	$U_{eq}$ (Å <sup>2</sup> )	Occupancy
La(1)	1a	0	0	0	0.0177(3)	1.0
La(2)	2d	1/3	2/3	1/2	0.0172(2)	1.0
Ni(1)	6l	0.18159(5)	2x	0	0.0175(3)	1.0
Mn(1)	6k	0.2985(1)	0	1/2	0.0178(4)	1.0
Mn(2)	3f	1/2	0	0	0.0176(5)	1.0
$R_{int} = 12.9\%$		Electron density residuals $\pm 1.5 \text{el./\AA}^3$				
$R_F^2 = 5.3\%$	$wR_F = 2.3\%$	$N_{meas}^a = 246$ , $N_{unique}^b = 146$				GoF = 1.06
Anisotropic displacement amplitudes						
	$U_{11}$	$U_{22}$	$U_{33}$	$U_{12}$	$U_{13}$	$U_{23}$
La(1)	2U12	2U12	0.0188(6)	0.0086(2)	0	0
La(2)	2U12	2U12	0.0182(5)	0.0084(1)	0	0
Ni(1)	0.0177(4)	2U12	0.0156(6)	0.0100(2)	0	0
Mn(1)	0.0209(4)	2U12	0.0142(7)	0.0086(2)	0	0
Mn(2)	0.0170(5)	2U12	0.0182(9)	0.0091(3)	0	0

Space group  $P6/mmm$ ,  $a=9.2099(9)$ ,  $c=4.1892(4)$  Å.

<sup>a</sup> Number of measured reflections.

<sup>b</sup> Number of unique reflections.

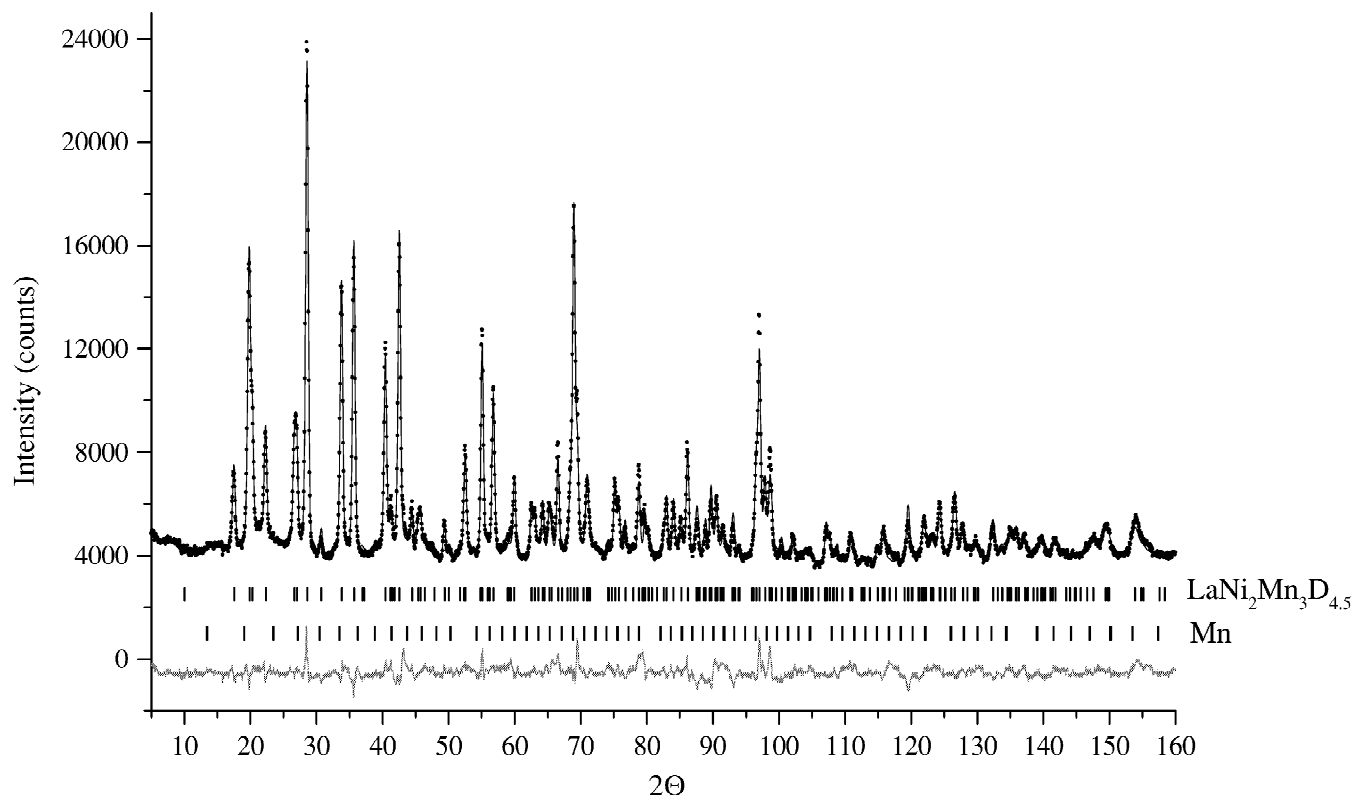


Fig. 3. Observed (points), calculated (line) and difference (bottom line) neutron diffraction patterns of  $\text{La}_{1.04}\text{Ni}_2\text{Mn}_3\text{D}_{4.6}$  (sample I) measured on HRPT (PSI,  $\lambda = 1.494 \text{ \AA}$ ). Vertical lines indicate Bragg peak position of the contributing phases  $\text{LaNi}_2\text{Mn}_3\text{D}_{4.6}$  (97%) and Mn (3%).

rich main phase, some Mn and traces of  $\text{La}_2\text{O}_3$  (0.3 wt.%). The refinements were performed along similar lines as for sample I. A total of 30 parameters were refined (three scale, seven profile and 20 atomic) while the displacement parameters of the five deuterium sites were constrained to be equal. The patterns are represented in Fig. 4 and the refinement results are summarised in Table 2. Interestingly, despite the anisotropic lattice expansion of the main phase (deuterides:  $c/a = 0.4433$  (I),  $0.4375$  (II); alloy  $\text{La}_{1.04}\text{Ni}_2\text{Mn}_3$ :  $c/a = 0.4543$ ) no significant anisotropic diffraction line broadening appeared. This contrasts with the hydrides of  $\text{LaNi}_5$  and most of their derivatives that show strongly broadened ( $hk0$ ) reflections [9].

### 3. Results and discussion

#### 3.1. Intermetallic compound

In contrast to  $\text{LaNi}_3\text{Mn}_2$  that crystallises with a partially disordered  $\text{CaCu}_5$  type structure [2]  $\text{LaNi}_2\text{Mn}_3$  crystallises with an ordered  $\text{YNi}_2\text{Al}_3$  type structure. Both structures are related as far as their hexagonal cell parameters are concerned ( $a_{\text{YNi}_2\text{Al}_3} = \sqrt{3} \times a_{\text{CaCu}_5}$ ,  $c_{\text{YNi}_2\text{Al}_3} = c_{\text{CaCu}_5}$ ,

$V_{\text{YNi}_2\text{Al}_3} = 3V_{\text{CaCu}_5}$ ), but differ with respect to their metal atom substructures, in particular that of lanthanum. In fact, the La positions in  $\text{LaNi}_2\text{Mn}_3$  ( $\text{YNi}_2\text{Al}_3$  type) can be derived from those in  $\text{LaNi}_3\text{Mn}_2$  ( $\text{CaCu}_5$  type) by displacing one out of three La atoms along  $1/2c$  (for a comparison between a  $\text{CaCu}_5$  type structure and a  $\text{YCo}_3\text{Ga}_2$  type structure which is a substitution variant of the  $\text{YNi}_2\text{Al}_3$  type structure, see Ref. [10]). As a consequence, the Ni and Mn atoms in the vicinity of the displaced La sites are able to relax and create atomic environments that differ significantly between both structure types. In  $\text{LaNi}_3\text{Mn}_2$  ( $\text{CaCu}_5$  type) the partially disordered Ni/Mn substructure consists of two mixed Ni/Mn sites that have coordination number  $\text{CN} = 12$  and shortest bond distances that are relatively similar for both sites ( $\text{Ni-Mn(Ni)} = 2.56 \text{ \AA}$ ,  $\text{Mn(Ni)-Mn(Ni)} = 2.59 \text{ \AA}$  [2]). In  $\text{LaNi}_2\text{Mn}_3$  ( $\text{YNi}_2\text{Al}_3$  type) the ordered Ni/Mn substructure consists of two Mn sites having  $\text{CN} = 12$  and one Ni site having  $\text{CN} = 11$ , and the shortest bond distances differ between these sites ( $\text{Ni-Mn} = 2.55 \text{ \AA}$ ,  $\text{Mn-Mn} = 2.75 \text{ \AA}$ ) as expected from atomic size considerations ( $R_{\text{Ni}} = 1.246$ ,  $R_{\text{Mn}} = 1.304 \text{ \AA}$ ). Altogether, these structural differences lead to rather different atomic environments in both hydride structures and thus to different hydrogenation properties (see Section 3.3).

Table 2

Structure refinement results on polycrystalline La<sub>1.04</sub>Ni<sub>2</sub>Mn<sub>3</sub>D<sub>4.6</sub> (sample **I**, first line) and La<sub>1.04</sub>Ni<sub>2</sub>Mn<sub>3</sub>D<sub>5.6</sub> (sample **II**, second line); e.s.d.s in parentheses

Atom	Site	x	y	z	B (Å <sup>2</sup> )	Occupancy
Phase 1:						
LaNi <sub>2</sub> Mn <sub>3</sub> D <sub>4.6</sub> : space group <i>P6/mmm</i> , refined phase content ~97 wt.%, a = 9.7125(2), c = 4.3057(1) Å, ΔV/V <sup>a</sup> = 14.7%						
LaNi <sub>2</sub> Mn <sub>3</sub> D <sub>5.6</sub> : space group <i>P6/mmm</i> , refined phase content ~93 wt.%, a = 9.8379(2), c = 4.3038(1) Å, ΔV/V <sup>a</sup> = 17.7%						
La1	1a	0	0	0	1.15(9) 0.81(6)	1.0
La2	2d	1/3	2/3	1/2	1.08(5) B <sub>La1</sub>	1.0
Ni1	6l	0.1841(2) 0.1847(3)	2x	0	1.78(3) 1.95(5)	1.0
Mn1	6k	0.2899(5) 0.2856(7)	0	1/2	1.95(8) 2.0(1)	1.0
Mn2	3f	1/2	0	0	1.7(1) 1.2(1)	1.0
D1	6m	0.072(1) 0.068(1)	2x	0.5	2.4(2) 3.04(8)	0.227(5) 0.288(7)
D2	3g	0.5	0	0.5	2.38(9) B <sub>D1</sub>	0.987(7) 1.00(1)
D3	6j	0.7440(6) 0.7458(6)	0	0	2.9(1) B <sub>D1</sub>	0.538(7) 0.68(1)
D4	12o	0.8003(6) 0.7981(5)	2x	0.630(2) 0.643(2)	2.1(2) B <sub>D1</sub>	0.164(3) 0.246(6)
D5	12p	0.5415(5) 0.4596(6)	0.3346(6) 0.6675(7)	0.0 0.0	2.00(8) B <sub>D1</sub>	0.351(3) 0.413(6)
R <sub>Bragg</sub> = 8.49%      N <sub>ref</sub> <sup>b</sup> = 205, 5.65%                      109,                      32 variables						
Phase 2:						
Mn (α-Mn type structure), space group <i>I43m</i> , a = 8.9474(–) Å (refined phase content ~3 (7) wt.%)						
R <sub>Bragg</sub> = 24.2%      N <sub>ref</sub> <sup>b</sup> = 110 18.7%                      57						
R <sub>p</sub> = 16.8%      R <sub>wp</sub> = 14.4%      Chi <sup>2</sup> = 7.91 13.8                      12.3                      5.71						

<sup>a</sup> Relative volume increase during deuteration.<sup>b</sup> Number of reflections.

### 3.2. Deuterides

As expected, the main phase in sample **I** (LaNi<sub>2</sub>Mn<sub>3</sub>D<sub>4.6</sub>) contains less deuterium than in sample **II** (LaNi<sub>2</sub>Mn<sub>3</sub>D<sub>5.6</sub>), and the refined deuterium contents (4.58(6) and 5.57(9) D/f.u., respectively) are slightly inferior than, but consistent with those measured for the hydride samples on the microbalance (~6 H/f.u). As shown in Fig. 5 deuterium occupies five different interstices, one octahedral coordinated site [La<sub>2</sub>Mn<sub>4</sub>] with full occupancy, and three tetrahedral coordinated sites [La<sub>2</sub>Mn<sub>2</sub>], [La<sub>2</sub>NiMn] and [LaMn<sub>2</sub>Ni], and a deformed square pyramidal coordinated site [LaMn<sub>2</sub>Ni<sub>2</sub>] with partial occupancies. The shapes of these interstices differ significantly from those occupied in CaCu<sub>5</sub> type hydrides AB<sub>5</sub>H<sub>x</sub> that have tetrahedral ([A<sub>2</sub>B<sub>2</sub>], [AB<sub>3</sub>], [B<sub>4</sub>]) and octahedral ([A<sub>2</sub>B<sub>4</sub>]) but no square-pyramidal metal coordinations. The metal–deuterium bond distances (Table 3) are in the usual range for intermetallic hydrides [11], and the

D–D distances (Table 4) and D site occupancies are consistent with repulsive D–D interaction (D–D > 2.1 Å). As can be seen from the radii of the various metal atom interstices (see R<sub>site</sub> in Table 4) they are all bigger than 0.4 Å, in agreement with Westlake's model [12]. Thus, from a purely geometric point of view the maximum deuterium content possible in this series of compounds is 8 D/f.u.

### 3.3. Hydrogenation properties

LaNi<sub>2</sub>Mn<sub>3</sub> absorbs reversibly up to 5.6 H/f.u. near ambient conditions (60 °C). Thus its maximum hydrogen capacity exceeds that of the end member of the LaNi<sub>5-x</sub>Mn<sub>x</sub> (CaCu<sub>5</sub> type) series (LaNi<sub>3</sub>Mn<sub>2</sub>: 4.8 H/f.u. at 60 °C [2]) and those of other systems showing a structural change from CaCu<sub>5</sub> type to YNi<sub>2</sub>Al<sub>3</sub> type structure such as neodymium-based NdNi<sub>5-x</sub>Al<sub>x</sub> (CaCu<sub>5</sub> type: x = 0.5, 1, 1.5; YNi<sub>2</sub>Al<sub>3</sub> type: x = 1.89–2.97; maximum H content 1.4 H/f.u. at x = 1.89 under 50 bar at 20 °C, activated at

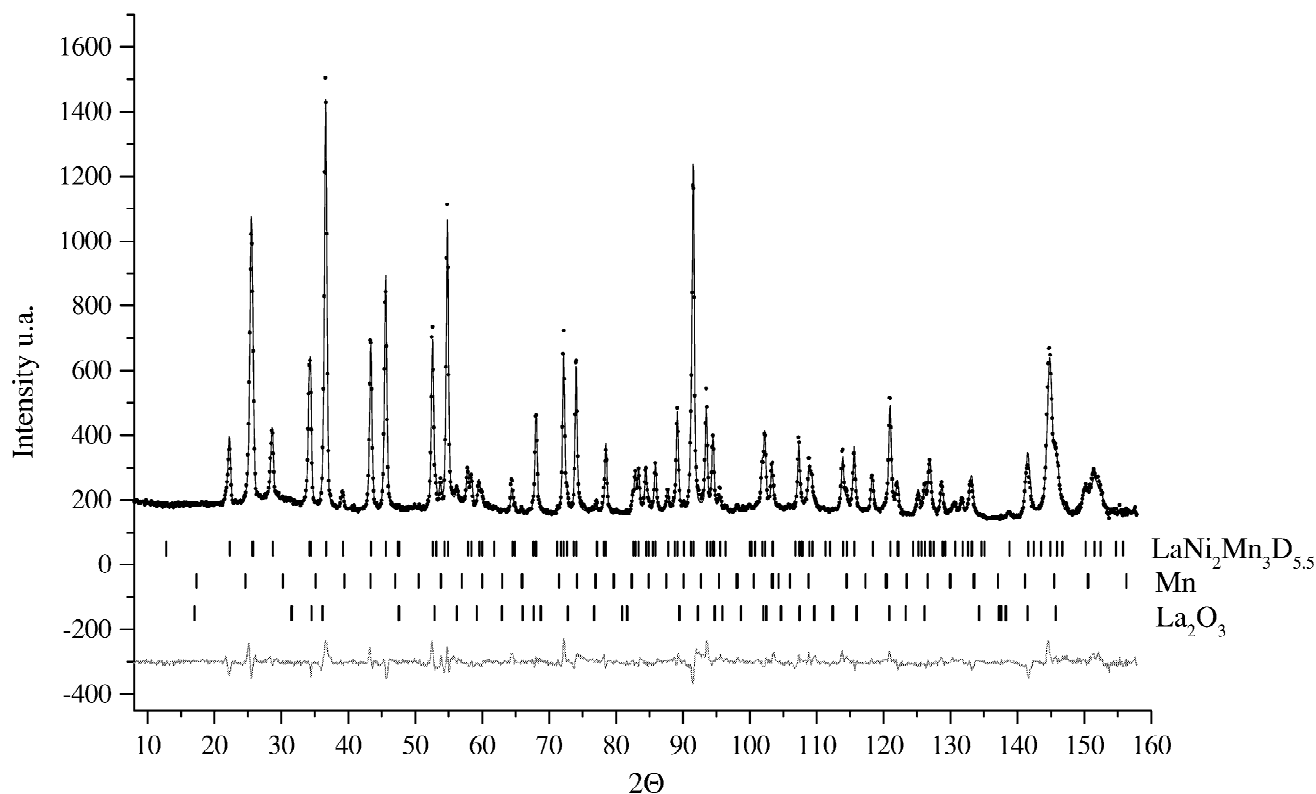


Fig. 4. Observed (points), calculated (line) and difference (bottom line) neutron diffraction pattern of  $\text{La}_{1.04}\text{Ni}_2\text{Mn}_3\text{D}_{5.6}$  (sample **II**) measured on D1A (ILL,  $\lambda=1.9114$  Å). Vertical lines indicate Bragg peak position of the contributing phases  $\text{LaNi}_2\text{Mn}_3\text{D}_{5.6}$  (92.5%), Mn (3%) and  $\text{La}_2\text{O}_3$  (0.5%).

300 °C [13]), or gadolinium-based  $\text{GdNi}_3\text{Al}_2$  (1.2H/f.u., 50 bar at 20 °C, activated at 300 °C) [14] and  $\text{GdNi}_{5-x}\text{Ga}_x$  ( $x=2.5$ : no significant hydrogen absorption up to 427 °C and 200 bar [15],  $x=2-3$ : inert up to 100 bar and 400 °C [16]). As to the hydrogen plateaus, that of  $\text{LaNi}_2\text{Mn}_3$  (~1

bar at 60 °C) is relatively well developed and in a more useful pressure range than that of  $\text{LaNi}_3\text{Mn}_2$  ( $\sim 10^{-5}$  bar at 60 °C [2]). On the other hand, in the aluminium substituted series  $\text{NdNi}_{5-x}\text{Al}_x$  compositions within the  $\text{CaCu}_5$  type structure domain (i.e., at low Al contents  $0 \leq x \leq 1.5$ ) show relatively wide plateaus that decrease with aluminium content, while compositions within the  $\text{YNi}_2\text{Al}_3$  type structure domain (i.e., at high Al contents  $1.89 \leq x \leq 2.97$ ) show no plateaus and small capacities ( $\text{NdNi}_{2.6}\text{Al}_{2.4}$ : 1.1 H/f.u. [13]). Finally, the kinetics of  $\text{LaNi}_2\text{Mn}_3$  is relatively slow at the beginning of the hydrogenation reaction but becomes rather fast once the reaction has started (see insert of Fig. 1), which indicates that it can be improved by activation. The calculated hydrogen densities of  $\text{LaNi}_2\text{Mn}_3\text{H}_6$  are 1.42 wt.% and  $82.5 \text{ g H}_2 \text{ l}^{-1}$ .

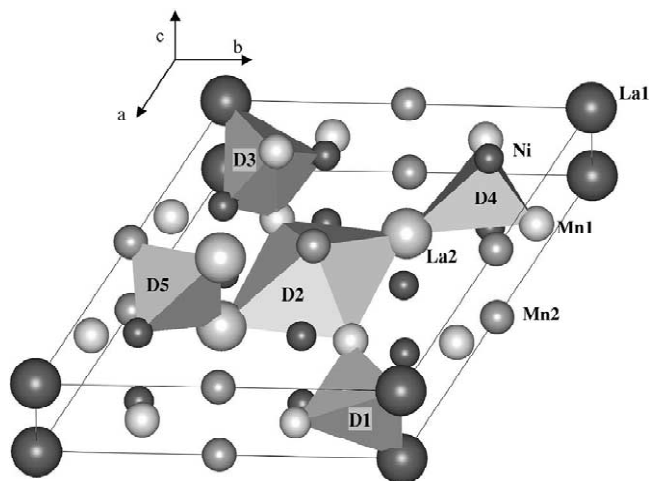


Fig. 5. Metal coordinations of deuterium sites in hexagonal  $\text{LaNi}_2\text{Mn}_3\text{D}_x$  ( $x=4.6, 5.6$ ). For clarity, only one representative of each site is drawn. Site symmetries: D1,  $\text{mm}2$ ; D2,  $\text{mmm}$ ; D3,  $\text{m}2\text{m}$ ; D4,  $\text{.m.}$ ; D5,  $\text{m.}$ ; large atoms, La; small dark grey atoms, Ni; medium light grey atoms, Mn1; medium dark grey atoms, Mn<sub>2</sub>.

#### 4. Conclusions

$\text{LaNi}_2\text{Mn}_3$  is a new intermetallic compound the structure and hydrogenation properties of which are distinctly different from those of  $\text{LaNi}_3\text{Mn}_2$  having similar composition. The relatively abrupt changes of hydrogenation properties as a function of composition are attributed to the structural differences between the alloys that lead to different hydrogen environments and thus different metal–hydrogen interactions in the hydrides. The compound has

Table 3

Metal coordinations, coordination numbers (CN), and interatomic distances<sup>a</sup> in LaNi<sub>2</sub>Mn<sub>3</sub>D<sub>4.6</sub>, LaNi<sub>2</sub>Mn<sub>3</sub>D<sub>5.6</sub> and LaNi<sub>2</sub>Mn<sub>3</sub>; e.s.d.s in parentheses

Central atoms	CN	Coordinated	LaNi <sub>2</sub> Mn <sub>3</sub> D <sub>4.6</sub>	LaNi <sub>2</sub> Mn <sub>3</sub> D <sub>5.6</sub>	LaNi <sub>2</sub> Mn <sub>3</sub>
			<i>a</i> = 9.7125(2) Å <i>c</i> = 4.3057(1) Å distances (Å)	<i>a</i> = 9.8379(2) Å <i>c</i> = 4.3038(1) Å distances (Å)	<i>a</i> = 9.2099(9) Å <i>c</i> = 4.1892(4) Å distances (Å)
La1 (1 <i>a</i> )	18	12Mn1	3.544(4)	3.540(5)	3.456(1)
		6Ni1	3.097(2)	3.147(3)	2.897(1)
La2 (2 <i>d</i> )	18	6Mn1	3.467(3)	3.538(6)	3.242(1)
		6Ni1	3.307(1)	3.323(2)	3.201(1)
		6Mn2	3.5347(1)	3.5629(1)	3.3844(2)
Mn1 (6 <i>k</i> )	12	2 Mn1	2.816(5)	2.810(5)	2.749(2)
		4 Ni1	2.655(1)	2.667(2)	2.558(1)
		2 Mn2	2.966(3)	3.013(5)	2.798(1)
		2 La2	3.467(3)	3.537(4)	3.242(1)
		2 La1	3.544(4)	3.539(6)	3.456(1)
Ni1 (6 <i>l</i> )	11	4 Mn1	2.655(1)	2.667(4)	2.558(1)
		2 Mn2	2.669(2)	2.700(3)	2.548(1)
		1 La1	3.097(2)	3.147(3)	2.897(1)
		2 La2	3.307(1)	3.324(2)	3.201(1)
		2 Ni1	3.097(2)	3.147(4)	2.897(1)
Mn2 (3 <i>f</i> )	12	4 Mn1	2.966(3)	3.013(5)	2.798(1)
		4 Ni1	2.669(2)	2.700(3)	2.548(1)
		4 La2	3.5347(1)	3.5629(1)	3.384(1)
D1 (6 <i>m</i> )	4	2La1	2.470(4)	2.442(6)	
		2Mn1	1.871(9)	1.90(2)	
D2 (3 <i>g</i> )	6	2La2	2.803(3)	2.841(1)	
		2Mn1	2.037(4)	2.109(6)	
		2Mn2	2.153(1)	2.152(1)	
D3 (6 <i>j</i> )	5	1La1	2.486(6)	2.501(6)	
		2Mn1	2.178(1)	2.174(1)	
		2Ni1	1.561(2)	1.590(3)	
D4 (12 <i>o</i> )	4	1La2	2.316(5)	2.322(5)	
		2Mn1	1.772(6)	1.835(5)	
		1Ni1	1.616(9)	1.563(8)	
D5 (12 <i>p</i> )	4	2La2	2.476(2)	2.483(3)	
		1Mn2	1.841(5)	1.878(6)	
		1Ni1	1.584(5)	1.581(6)	

<sup>a</sup> D–Ni(Mn) cut-off distance <2.7(2.4) Å.

Table 4

Shortest distances between D atom sites and interstitial hole size ( $R_{\text{site}}$ ) in LaNi<sub>2</sub>Mn<sub>3</sub>D<sub>4.6</sub> and LaNi<sub>2</sub>Mn<sub>3</sub>D<sub>5.6</sub>; e.s.d.s in parentheses

Atom (site)	LaNi <sub>2</sub> Mn <sub>3</sub> D <sub>4.6</sub>			LaNi <sub>2</sub> Mn <sub>3</sub> D <sub>5.6</sub>		
	Neighbours	Distances (Å)	$R_{\text{site}}$ <sup>a</sup> (Å)	Neighbours	Distances (Å)	$R_{\text{site}}$ <sup>a</sup> (Å)
D1 (6 <i>m</i> )	2 D1	1.21(1)	0.58	2 D1	1.15(2)	0.58
	2 D1	2.10(1)		2 D1	2.00(2)	
D2 (3 <i>g</i> )	8 D4	2.632(5)	0.74	8 D4	2.665(5)	0.81
D3 (6 <i>j</i> )	4 D4	2.353(7)	0.36	4 D4	2.355(7)	0.39
D4 (12 <i>o</i> )	1 D4	1.12(1)	0.44	1 D4	1.23(1)	0.46
				2 D5	2.02(1)	
D5 (12 <i>p</i> )	1 D5	1.20(2)	0.54	1 D5	1.23(1)	0.55
	1 D5	1.24(2)		1 D5	1.25(1)	
				1 D4	2.02(1)	

<sup>a</sup> Calculated from atomic radii  $R_{\text{La}} = 1.877$  Å,  $R_{\text{Mn}} = 1.304$  Å,  $R_{\text{Ni}} = 1.246$  Å [17] within the hard sphere approximation.

relatively good hydrogen storage efficiencies and fast kinetics and thus is useful for hydrogen storage applications. Its discovery underlines the usefulness of modelling the structural stability of intermetallic compounds for the search of new hydrogen storage materials.

### Acknowledgements

The authors thank the staff of the Swiss Norwegian beamline at ESRF (Grenoble), C. Ritter (D1A, ILL, Grenoble) and D. Sheptyakov (HRPT, PSI, Villigen) for help with collecting the diffraction patterns. Thanks are also due to R. Cerny (Geneva) and V. Favre-Nicolin (ESRF, Grenoble) for discussions and help with the newly developed computer program FOX. This work was supported by the Swiss National Science Foundation and the Swiss Federal Office of Energy.

### References

- [1] F. Cuevas, J.-M. Joubert, M. Latroche, A. Percheron-Guégan, *Appl. Phys. A* 72 (2001) 225–238.
- [2] C. Lartigue, A. Percheron-Guegan, J.C. Achard, F. Tasset, *Rare earth in modern science and technology, Rare Earths Res. Conf. 2* (1980) 585–591.
- [3] Ya.M. Kal'chak, O.I. Bodak, E.I. Gladyshevskiy, *Russian Metallurgy*, Translated from *Izvestiya Akademii Nauk SSSR, Metaly* (5) (1980) 217–221.
- [4] L. Guénee, PhD Thesis No. 3341, University of Geneva (2002).
- [5] S.R. Hall, D.J. du Boulay, R. Olthof-Hazekamp, Eds. *Xtal3.7 System*. University of Western Australia (2000).
- [6] J.L.C. Daams, P. Villars, J.H.N. Van Vucht, in: *Atlas of Crystal Structure Types For Intermetallic Phases*, ASM International, Materials Park, OH 44073, 1991.
- [7] V. Favre-Nicolin, R. Cerny, *J. Appl. Cryst.* (2002) submitted, see also <http://objcryst.sourceforge.net>
- [8] J. Rodríguez-Carvajal, in: *Abstract of the Satellite Meeting on Powder Diffraction, Congress of the International Union of Crystallography, Toulouse, France, 1990*, p. 127. Fullprof Program, version 3.5d Oct 98-LLB-JRC, 1998.
- [9] R. Cerny, J.-M. Joubert, M. Latroche, A. Percheron-Guégan, K. Yvon, *J. Appl. Crystallogr.* 33 (2000) 997.
- [10] M.A. Fremy, D. Gignoux, *J. Less-Common Met.* 106 (1985) 251–255.
- [11] K. Yvon, P. Fischer, *Topics in applied physics*, in: L. Schlapbach (Ed.), *Hydrogen in Intermetallic Compounds I*, Vol. 63, Springer, New York, 1988, p. 87.
- [12] D.G. Westlake, *J. Less-Common Met.* 90 (1983) 251.
- [13] J.-L. Bobet, S. Pechev, B. Chevalier, B. Darriet, *J. Alloys Comp.* 267 (1998) 136–141.
- [14] S. Pechev, J.-L. Bobet, B. Chevalier, B. Darriet, F. Weill, *J. Solid State Chem.* 150 (2000) 62–71.
- [15] Z. Blazina, B. Sorgic, A. Drasner, *J. Phys.: Condens. Matter* 11 (1999) 3105–3114.
- [16] G.I. Miletic, A. Drasner, Z. Blazina, *J. Alloys Comp.* 296 (2000) 170–174.
- [17] E. Teatum, K. Gschneider, J. Waber (1960), LA-2345, US Department of Commerce, Washington, DC. (cf. book: W.B. Pearson, *The Crystal Chemistry and Physics of Metals and Alloys*, p. 151).